Vol 14 No 1, January 2005
1009-1963/2005/14(01)/0102-08

Chinese Physics

© 2005 Chin. Phys. Soc.
and IOP Publishing Ltd

Spontaneous emission spectrum of a three-level atom embedded in photonic crystal*

Liu Guo-Qiang(刘国强), Wang Jian(王 健), and Zhang Han-Zhuang(张汉壮)†

College of Physics, Jilin University, Changchun 130023, *China*

(Received 8 October 2003; revised manuscript received 18 August 2004)

The two models of three-level (one upper level and two lower levels, or two upper levels and one lower level) atom embedded in a double-band photonic crystal are adopted. The atomic transitions from the upper levels to the lower levels are assumed to be coupled by the same reservoir which are respectively the isotropic photonic band gap (PBG) modes, the anisotropic PBG modes and the free vacuum modes. The effects of the fine structure of the atomic ground state levels in the model with one upper level and two lower levels, and the quantum interferences in the model with two upper levels and one lower level on the spontaneous emission spectrum of an atom are investigated in detail. Most interestingly, it is shown that new spontaneous emission lines are produced from the fine splitting of atomic ground state levels in the isotropic PBG case. The quantum interferences induce additional narrow spontaneous lines near the transition from the empty upper level to the lower level.

Keywords: photonic band gap, quantum interference, spontaneous emission spectrum
PACC: 3200, 3270, 4250

1. Introduction

More recently, the study of the spontaneous emission of an atom in the free vacuum reservoirs has attracted considerable attention. The interests in this subject stem from many remarkable phenomena resulting from quantum interference in spontaneous emission: for example, very narrow absorption and fluorescence spectra,[1−6] population trapping in a degenerate system,[7,8] fluorescence quenching in the free space,[5,9,10] phase-dependent line shapes,[11,12] lasing without inversion,[13] and others.[14−23] It is well known that the spontaneous emission depends not only on the properties of the excited atomic system but also on the nature of the surrounding environment—also called reservoirs.[24,25] The environment includes the types of both Markov environment, for example free vacuum modes (reservoirs), and non-Markov environment. The spontaneous emission spectrum of an atom coupled to a non-Markov environment will obviously exhibit different properties compared to that of one coupled to a Markov environment. Photonic band gap (PBG) structures have been shown to have a density of states (DOS) of emission field different from that of free-space vacuum field.[24−27] The study of quantum and nonlinear optical phenomena for archetypes of atoms embedded in such PBG materials leads to the prediction of many interesting effects: for example, localization of light,[28,29] photon–atom bound states,[24,25,28,30] suppression and even complete cancellation of spontaneous emission,[31,32] enhancement of spontaneous emission,[33−37] electro-magnetically induced transparency and other phenomena.[38−46]

As far as we know, for an atom embedded in a photonic crystal most studies reported to date have focused on the population involution and distribution in upper levels[24,25,28] and the spectral components in spontaneous emission fields.[33−36] Knight and his co-workers have investigated transparency and coherent phenomena in photonic crystals in the Λ-type model where one transition interacts with free vacuum modes and the other interacts with modes near the PBG's edges.[38,39] Focusing on the quantum interference of an atom without externally driving coherent laser field, Zhou and Swain,[1,2] and Zhu[3] have independently reported the quantum interference in spontaneous emission spectrum and in probe absorption

*Project supported by the Scientific Research Foundation for the Returned Overseas Chinese Scholars, State Education Ministry, and the Innovative Research Foundation of Jilin University
†Corresponding author: Hzzhang@email.jlu.edu.cn

spectrum of an atom coupled to vacuum space reservoirs. In our previous papers,[47−49] we have studied in detail the spontaneous emission spectrum of the V-type three-level and the double V-type four-level atoms in a double-band photonic crystal for the first time. In the papers, we assumed that the atomic transitions from the two upper levels to the two lower levels were coupled synchronously by PBG modes and by free vacuum modes. As a result, the ground state levels of an atom have acquired a superfine energy level structure, leading to greater versatility from the point of view of practice. Furthermore, it is recognized as an universal feature that atomic transitions from the upper levels to the lower ground state levels are confined to coupling by the same reservoir. In this paper, we adopt two types of models of a three-level atom in a double-band photonic crystal described respectively by isotropic and anisotropic dispersion relations at the band edges. One includes one upper level and two lower levels, the other includes two upper levels and one lower level. The atomic transitions from the upper levels to the lower levels are restricted to coupling by the same reservoir without loss of generality, which we assume in turn to be the isotropic PBG modes, the anisotropic PBG modes and the free vacuum modes. The effects of the fine structure of the ground state levels on the spontaneous emission spectrum of an atom are studied in the first model. The quantum interferences in the three cases are analysed and compared with each other in the second model. In Section 2, we derive the equations for describing the spontaneous emission spectrum of the three-level atom in a photonic crystal in the case of the two models. The general calculations and analyses are presented in Section 3. The major conclusions are summarized in Section 4.

2. Equations for the spontaneous emission spectrum in the two models

Consider a three-level atom with upper level $|2\rangle$ and lower levels $|1\rangle$ and $|0\rangle$ as shown in Fig.1(a) as the first model, or a three-level atom with upper levels $|3\rangle$ and $|2\rangle$ and lower level $|0\rangle$ as shown in Fig.1(b) as the second model. We assume that the transitions from the two upper levels to the lower levels are coupled by the same reservoir, which are respectively isotropic PBG modes, anisotropic PBG modes and free vacuum modes. The dispersion relations near the photonic band edges are approximated by[24]

$$\omega_k = \omega_{c1} - A_1(k-k_0)^2, \quad k < k_0,$$
$$\omega_k = \omega_{c2} + A_2(k-k_0)^2, \quad k > k_0, \tag{1}$$

$$\omega_k = \omega_{c1} - A_1|(\vec{k}-\vec{k}_0)|^2, \quad |\vec{k}| < |\vec{k}_0|,$$
$$\omega_k = \omega_{c2} + A_2|(\vec{k}-\vec{k}_0)|^2, \quad |\vec{k}| > |\vec{k}_0|. \tag{2}$$

for isotropic dispersion relation and anisotropic dispersion relation, respectively. Here $A_n \approx \omega_{cn}/k_0^2$ $(n = 1, 2)$. ω_{c1} and ω_{c2} are the upper and lower frequencies at the edges of the forbidden gap, respectively. The Hamiltonian describing the dynamics of

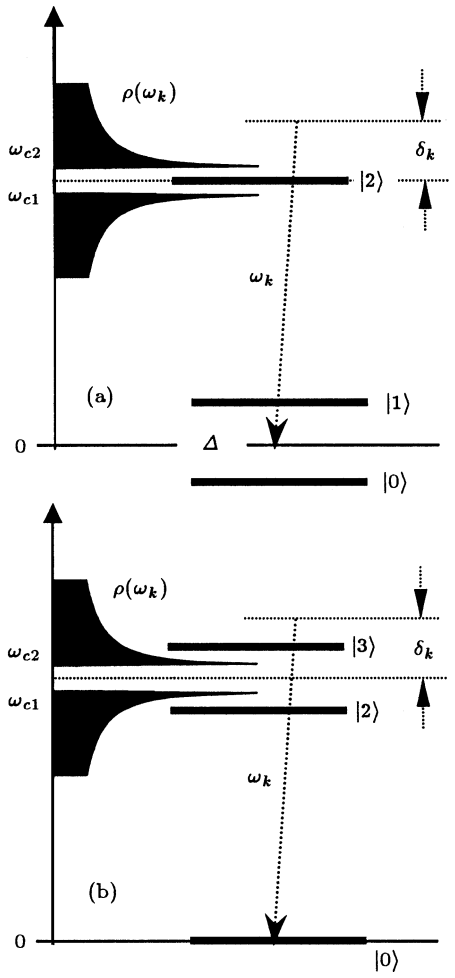


Fig.1. Schematic diagram of the three-level atom in double photonic band structure. $\rho(\omega_k)$ denotes the density of states of the isotropic PBG modes. ω_{c2} and ω_{c1} are the upper and lower frequencies of the forbidden gap, respectively. δ_k is the detuning of frequency of radiation field (ω_k) in the middle of the forbidden gap. It is assumed that the transitions from the upper levels $|3\rangle$ and $|2\rangle$ to the lower levels $|1\rangle$ and $|0\rangle$ are coupled by the same reservoir. (a) For the case of one upper level and two lower levels. Δ denotes the width between the lower two levels. (b) For the case of two upper levels and one lower level.

this system in the interaction picture and the rotating wave approximation can be written as

$$\begin{aligned} H_i =&\hbar\sum_{ke}(g_{ke}^{20}a_{ke}^{+}b_0^{+}b_2\mathrm{e}^{\mathrm{i}\mu_k^{20}t} \\ &+ g_{ke}^{21}a_{ke}^{+}b_1^{+}b_2\mathrm{e}^{\mathrm{i}\mu_k^{21}t}+\mathrm{C.C.}), \\ H_i =&\hbar\sum_{ke}(g_{ke}^{30}a_{ke}^{+}b_0^{+}b_3\mathrm{e}^{\mathrm{i}\mu_k^{30}t} \\ &+ g_{ke}^{20}a_{ke}^{+}b_0^{+}b_2\mathrm{e}^{\mathrm{i}\mu_k^{20}t}+\mathrm{C.C.}) \end{aligned} \tag{3}$$

for the first model and the second model, respectively. Where C.C. denotes conjugate for the other two items in the bracket; and b_i^{+}, b_i (i=0,1,2,3) are creation and annihilation operators for an atom in level i, respectively; a_{ke}^{+} (a_{ke}) is the creation (annihilation) operator for the kth PBG mode with frequency ω_k; g_{ke}^{jn} (j=2,3, n=0,1) is the frequency-dependent coupling constant between the atomic transitions $|j\rangle$-$|n\rangle$. More precisely,

$$\begin{aligned} g_{ke}^{jn} &= (\omega_{jn}d_{jn}/\hbar)(\hbar/2\varepsilon_0\omega_k V)^{1/2}\vec{e}_{ke}\cdot\vec{d}_{jn}, \\ \mu_k^{jn} &= \omega_k-\omega_{jn}, \\ &(j=2,3,n=0,1), \end{aligned} \tag{4}$$

where $\boldsymbol{d}_{jn}$ (j=2,3, n=0,1) is the atomic dipole moment unit vector for the transition $|j\rangle$-$|n\rangle$. $\boldsymbol{e}_{ke}$ (e=1,2) is the polarization unit vector of the radiation field, and V is the sample volume. The state vector of the system in the interaction picture can be written as

$$\begin{aligned} |\Psi(t)\rangle =&A_2(t)|2,\{0\}\rangle \\ &+\sum_{ke}A_{1ke}|1,\{ke\}\rangle \\ &+\sum_{ke}A_{0ke}|0,\{ke\}\rangle, \\ |\Psi(t)\rangle =&A_3(t)|3,\{0\}\rangle+A_2(t)|2,\{0\}\rangle \\ &+\sum_{ke}A_{0ke}|0,\{ke\}\rangle \end{aligned} \tag{5}$$

for the first model and the second model, respectively. Substituting Eq.(3) and Eq.(5) into the Schrödinger equation, we obtain

$$\begin{aligned} \frac{\mathrm{d}A_2(t)}{\mathrm{d}t} =&-\mathrm{i}\sum_{ke}g_{ke}^{21}\mathrm{e}^{-\mathrm{i}\mu_k^{21}t}A_{1ke}(t) \\ &-\mathrm{i}\sum_{ke}g_{ke}^{20}\mathrm{e}^{-\mathrm{i}\mu_k^{20}t}A_{0ke}(t), \\ \frac{\mathrm{d}A_{1ke}(t)}{\mathrm{d}t} =&-\mathrm{i}g_{ke}^{21}\mathrm{e}^{\mathrm{i}\mu_k^{21}t}A_2(t), \\ \frac{\mathrm{d}A_{0ke}(t)}{\mathrm{d}t} =&-\mathrm{i}g_{ke}^{20}\mathrm{e}^{\mathrm{i}\mu_k^{20}t}A_2(t), \end{aligned} \tag{6}$$

$$\begin{aligned} \frac{\mathrm{d}A_3(t)}{\mathrm{d}t} =&-\mathrm{i}\sum_{ke}g_{ke}^{30}\mathrm{e}^{-\mathrm{i}\mu_k^{30}t}A_{0ke}(t), \\ \frac{\mathrm{d}A_2(t)}{\mathrm{d}t} =&-\mathrm{i}\sum_{ke}g_{ke}^{20}\mathrm{e}^{-\mathrm{i}\mu_k^{20}t}A_{0ke}(t), \\ \frac{\mathrm{d}A_{0ke}(t)}{\mathrm{d}t} =&-\mathrm{i}g_{ke}^{30}\mathrm{e}^{\mathrm{i}\mu_k^{30}t}A_3(t)-\mathrm{i}g_{ke}^{20}\mathrm{e}^{\mathrm{i}\mu_k^{20}t}A_2(t), \end{aligned} \tag{7}$$

for the first model and the second model, respectively. Formally integrating and eliminating $A_{1\lambda e}(t)$ and $A_{0ke}(t)$ from Eq.(6) and Eq.(7), we obtain

$$\begin{aligned} \frac{\mathrm{d}A_2(t)}{\mathrm{d}t} =&-\int_0^t G_{22}^{k1}(t-t')A_2(t')\mathrm{d}t' \\ &-\int_0^t G_{22}^{k0}(t-t')A_2(t')\mathrm{d}t', \\ \frac{\mathrm{d}A_3(t)}{\mathrm{d}t} =&-\int_0^t G_{33}^{k0}(t-t')A_3(t')\mathrm{d}t' \\ &-\int_0^t G_{23}^{k0}(t-t')\mathrm{e}^{\mathrm{i}\omega_{32}t'}A_2(t')\mathrm{d}t', \end{aligned} \tag{8}$$

$$\begin{aligned} \frac{\mathrm{d}A_2(t)}{\mathrm{d}t} =&-\int_0^t G_{22}^{k0}(t-t')A_2(t')\mathrm{d}t' \\ &-\int_0^t G_{32}^{k0}(t-t')\mathrm{e}^{-\mathrm{i}\omega_{32}t'}A_3(t')\mathrm{d}t', \end{aligned} \tag{9}$$

for the first model and the second model, respectively, where

$$\begin{aligned} G_{jl}^{kn}(t-t') &= \sum_{ke}g_{ke}^{jn}g_{ke}^{ln}\mathrm{e}^{-\mathrm{i}\mu_k^{ln}(t-t')} \\ &(j,l=2,3,n=0,1) \end{aligned} \tag{10}$$

is the delayed Green functions which can be transformed into the following forms:[24]

$$\begin{aligned} G_{jl}^{kn}(t-t') =&\eta_{jl}^{kn}\sqrt{\beta_{jn}^{3/2}\beta_{ln}^{3/2}}\left\{\frac{\mathrm{e}^{\mathrm{i}[\delta_{lnc2}(t-t')-\pi/4]}}{\sqrt{\pi(t-t')}}\right. \\ &\left.+\frac{\mathrm{e}^{\mathrm{i}[\delta_{lnc1}(t-t')+\pi/4]}}{\sqrt{\pi(t-t')}}\right\}, \\ G_{jl}^{kn}(t-t') =&\eta_{jl}^{kn}\sqrt{\alpha_{jn}\alpha_{ln}}\left\{\frac{\mathrm{e}^{\mathrm{i}[\delta_{lnc2}(t-t')+\pi/4]}}{\sqrt{4\pi(t-t')^3}}\right. \\ &\left.+\frac{\mathrm{e}^{\mathrm{i}[\delta_{lnc1}(t-t')-\pi/4]}}{\sqrt{4\pi(t-t')^3}}\right\}, \\ G_{jl}^{kn}(t-t') =&\eta_{jl}^{kn}\sqrt{\gamma_{jn}\gamma_{ln}}\delta(t-t'), \\ &(j,l=2,3,n=0,1) \end{aligned} \tag{11}$$

for isotropic PBG, anisotropic PBG and free space reservoirs, respectively. The definitions of the parameters are

$$\begin{aligned} &\beta_{jn}^{3/2}=\frac{1}{4\pi\varepsilon_0}\frac{\omega_{jn}^2d_{jn}^2\omega_{c2}^{3/2}}{3\hbar c^3}, \quad \alpha_{jn}=\frac{1}{4\pi\varepsilon_0}\frac{\omega_{jn}^2d_{jn}^2\omega_{c2}^{1/2}}{3\hbar c^3}, \\ &\gamma_{jn}=\frac{1}{\pi\varepsilon_0}\frac{\omega_{jn}^3d_{jn}^2}{3\hbar c^3}, \quad (j,l=2,3,n=0,1). \end{aligned} \tag{12}$$

In Eq.(11), $\eta_{jl}^{kn} = \delta_{jl} + \eta_k^n(1-\delta_{jl})$, where δ_{jl} is the delta function, and $\eta_k^n = \frac{3}{8\pi}\int(\cos\varphi_{3n}^k\cos\varphi_{2n}^k + \cos\upsilon_{3n}^k\cos\upsilon_{2n}^k)\mathrm{d}\Omega$. Here $\{\varphi_{jn}^k, \upsilon_{jn}^k, \theta_{jn}^k\}$ (j=2,3, n=0,1) is the directional angles of the dipole moment unit vectors $\boldsymbol{d}_{jn}$ in a coordinate system defined by the unit vectors $\{\boldsymbol{e}_{k1}, \boldsymbol{e}_{k2}, \boldsymbol{k}\}$, and $\mathrm{d}\Omega$ is the solid angle element. It is seen that $\eta_k^n = 1.0$ when $\boldsymbol{d}_{jn}\cdot\boldsymbol{d}_{ln} = \pm 1$, and $\eta_k^n = 0$ when $\boldsymbol{d}_{jn}\cdot\boldsymbol{d}_{ln} = 0$. Otherwise, $0 < \eta_k^n < 1.0$. Therefore, the parameters $\eta_{22}^{kn} = \eta_{33}^{kn} = 1.0$ are independent of η_k^n. The parameter $\eta_{32}^{kn} = \eta_{23}^{kn}$ is the coherent coupling coefficient of the transitions between $|3\rangle - |n\rangle$ and $|2\rangle - |n\rangle$ coupled to the reservoir. When the dipole moments of the transitions from the two upper levels to one of the two lower levels are orthogonal, $\eta_{32}^{kn} = 0$, implying that there is no quantum interference between the transitions. When the dipole moments of the transitions are parallel or anti-parallel, $\eta_{32}^{kn} = 1.0$, implying that the quantum interference is maximal between the transitions. There are also two types of quantum interferences in this system similar to that mentioned in our previous papers.[47−49]

The spontaneous spectrum $S(\omega_k)$ of the atom is the Fourier transform of [3]

$$\begin{aligned}&\langle E^-(t+\tau)E^+(t)\rangle_{t\to\infty}\\ &= <\Psi(t)\Big|\sum_{k,k'}a_{ke}^+a_{k'e}\mathrm{e}^{\mathrm{i}\omega_k(t+\tau)}\mathrm{e}^{-\mathrm{i}\omega_{k'}t}\Big|\Psi(t)\Big\rangle_{t\to\infty}.\end{aligned} \tag{13}$$

Substituting Eq.(5) into Eq.(13), we have

$$\begin{aligned}&\langle E^-(t+\tau)E^+(t)\rangle_{t\to\infty}\\ &=\sum_{ke}A_{0ke}^*(\infty)A_{0ke}(\infty)\mathrm{e}^{\mathrm{i}\omega_k\tau}\\ &\quad+\sum_{ke}A_{1ke}^*(\infty)A_{1ke}(\infty)\mathrm{e}^{\mathrm{i}\omega_k\tau}\\ &=\int_{-\infty}^{+\infty}\mathrm{e}^{\mathrm{i}\omega_k\tau}d\omega_kD(\omega_k)\\ &\quad\times\int\sum_{e=1}^{2}[A_{0ke}^*(\infty)A_{0ke}(\infty)\\ &\quad+A_{1ke}^*(\infty)A_{1ke}(\infty)]\mathrm{d}\Omega,\end{aligned} \tag{14}$$

$$\begin{aligned}&\langle E^-(t+\tau)E^+(t)\rangle_{t\to\infty}\\ &=\sum_{ke}A_{0ke}^*(\infty)A_{0ke}(\infty)\mathrm{e}^{\mathrm{i}\omega_k\tau}\\ &=\int_{-\infty}^{+\infty}\mathrm{e}^{\mathrm{i}\omega_k\tau}d\omega_kD(\omega_k)\\ &\quad\times\int\sum_{e=1}^{2}[A_{0ke}^*(\infty)A_{0ke}(\infty)]\mathrm{d}\Omega\end{aligned} \tag{15}$$

for the first model and the second model, respectively. Here $D(\omega_k)$ is DOS of the radiation field, which can be derived as[24]

$$\begin{aligned}D(\omega_k)\sim&\frac{1.0}{\sqrt{\omega_k-\omega_{c2}}}\Theta(\omega_k-\omega_{c2})\\ &+\frac{1.0}{\sqrt{\omega_{c1}-\omega_k}}\Theta(\omega_{c1}-\omega_k)\\ D(\omega_k)\sim&\sqrt{\omega_k-\omega_{c2}}\Theta(\omega_k-\omega_{c2})\\ &+\sqrt{\omega_{c1}-\omega_k}\Theta(\omega_{c1}-\omega_k)\\ D(\omega_k)\sim&1.0\end{aligned} \tag{16}$$

for isotropic PBG, anisotropic PBG and free space reservoirs, respectively, where Θ is the Heaviside step function. From Eqs.(4), (6), (7), (12), (14) and (15), we have

$$\begin{aligned}S_(\omega_k)=&D(\omega_k)[P_{20}\widetilde{A}_2^*(s\to-\mathrm{i}\mu_k^{20})\widetilde{A}_2(s\to-\mathrm{i}\mu_k^{20})\\ &+P_{21}\widetilde{A}_2^*(s\to-\mathrm{i}\mu_k^{21})\widetilde{A}_2(s\to-\mathrm{i}\mu_k^{21})],\\ S_(\omega_k)=&D(\omega_k)[P_{30}\widetilde{A}_3^*(s\to-\mathrm{i}\mu_k^{30})\widetilde{A}_3(s\to-\mathrm{i}\mu_k^{30})\\ &+P_{20}\widetilde{A}_2^*(s\to-\mathrm{i}\mu_k^{20})\widetilde{A}_2(s\to-\mathrm{i}\mu_k^{20})]\\ &+D(\omega_k)\sqrt{P_{30}P_{20}}\eta_{32}^{k0}\\ &\times[\widetilde{A}_3^*(s\to-\mathrm{i}\mu_k^{30})\widetilde{A}_2(s\to-\mathrm{i}\mu_k^{20})\\ &+\widetilde{A}_3(s\to-\mathrm{i}\mu_k^{30})\widetilde{A}_2^*(s\to-\mathrm{i}\mu_k^{20})]\end{aligned} \tag{17}$$

for the first model and the second model, respectively. Here the definitions of P_{jn} (j=2,3, n=0,1) are

$$\begin{aligned}P_{jn}&=\beta_{jn}^{\frac{3}{2}},\\ P_{jn}&=\alpha_{jn},\\ P_{jn}&=\gamma_{jn}\end{aligned} \tag{18}$$

for isotropic PBG, anisotropic PBG and free vacuum modes. $\widetilde{A}_j(s)$ (j=2,3) is the Laplace transform of $A_j(t)$. Taking the Laplace transform of Eq.(8) and Eq.(9), we obtain

$$\widetilde{A}_2(s) = \frac{A_2(0)}{s+\widetilde{G}_{22}^{k0}(s)+\widetilde{G}_{22}^{k1}(s)} \tag{19}$$

for the first model, and

$$\begin{aligned}\widetilde{A}_3(s)&=\frac{M_4(s)A_3(0)-M_2(s)A_2(0)}{M_1(s)M_4-M_2(s)M_3(s)},\\ \widetilde{A}_2(s-\mathrm{i}\omega_{32})&=\frac{M_1(s)A_2(0)-M_3(s)A_3(0)}{M_1(s)M_4(s)-M_2(s)M_3(s)},\end{aligned} \tag{20}$$

where

$$\begin{aligned}M_1(s)&=s+\widetilde{G}_{33}^{k0}(s),\\ M_2(s)&=\widetilde{G}_{23}^{k0}(s),\\ M_3(s)&=\widetilde{G}_{32}^{k0}(s-\mathrm{i}\omega_{32}),\\ M_4(s)&=s-\mathrm{i}\omega_{32}+\widetilde{G}_{22}^{k0}(s-\mathrm{i}\omega_{32})\end{aligned} \tag{21}$$

for the second model. Here $\omega_{32} = \omega_{31} - \omega_{21}$ is the frequency difference between the upper two levels, $A_2(0)$ and $A_3(0)$ are the initial values of $A_2(t)$ and $A_3(t)$ respectively, and $\widetilde{G}_{jl}^{kn}(s)$ $(j,l$=2,3, n=0,1) is the Laplace transform of the delayed Green function in Eq.(11), which can be derived in the forms of

$$\begin{aligned}
\widetilde{G}_{jl}^{kn}(s) =& \eta_{jl}^{kn}\sqrt{\beta_{jn}^{3/2}\beta_{ln}^{3/2}}\left\{\frac{\mathrm{i}}{\sqrt{\mathrm{i}s+\delta_{lnc1}}}+\frac{1.0}{\sqrt{\mathrm{i}s+\delta_{lnc2}}}\right\},\\
\widetilde{G}_{jl}^{kn}(s) =& \eta_{jl}^{kn}\sqrt{\alpha_{jn}\alpha_{ln}}\{-\mathrm{i}\sqrt{\mathrm{i}s+\delta_{lnc1}}+\sqrt{\mathrm{i}s+\delta_{lnc2}}\},\\
\widetilde{G}_{jl}^{kn}(s) =& \eta_{jl}^{kn}\sqrt{\gamma_{jn}\gamma_{ln}},\\
& (j,l=2,3,n=0,1) \qquad (22)
\end{aligned}$$

for isotropic PBG, anisotropic PBG and free space reservoirs, respectively. Here the definitions of the detuning parameters are

$$\begin{aligned}
\mu_k^{j1} =& \mu_k^{j0}+\Delta;\\
\mu_k^{2n} =& \mu_k^{3n}+\omega_{32},\\
\mu_k^{3n} =& \delta_k-\frac{1}{2}\delta_{c2c1}-\delta_{3nc2},\\
\delta_{3nc2} =& \delta_{3c2}+\frac{1}{2}\Delta;\\
\delta_{2nc1} =& \delta_{2c1}-\frac{1}{2}\Delta,\\
\delta_{3nc1} =& \delta_{3nc2}+\delta_{c2c1};\\
\delta_{2nc2} =& \delta_{2nc1}-\delta_{c2c1},\\
& (j=2,3,n=0,1) \qquad (23)
\end{aligned}$$

where δ_{3c2} and δ_{2c1} are the differences between the upper levels 3 and 2 from the upper and the lower edges of the band gap, respectively. δ_k is the detuning of frequency of radiation field (ω_k) from the middle of the forbidden gap. δ_{c2c1} and Δ denote the width of the forbidden gap and splitting width of the lower two levels, respectively. The amplitudes A_{20} and A_{30} represent the initial probability of an atom occurring in the upper levels $|2\rangle$ and $|3\rangle$ respectively. The calculation of the spontaneous emission spectrum can be performed based on Eqs.(17) and (19)–(21), using the parameters defined in Eqs.(16), (18), (22) and (23). It is seen that there is no quantum interference in the first model, whereas the coherent parameter η_{32}^{kn} (n=0,1) in the second model is embodied not only in the Laplace transforms of the delayed Green functions, but also in the third and fourth terms (cross terms) of Eq.(17). The remarkable spontaneous emission spectrum features resulting from the splitting width (Δ) of ground state level and the interferences are discussed in the following section.

3. Results and discussion

3.1. Effects of splitting of lower levels on the spontaneous emission spectrum

For more realistic simulation of an atom, its ground state has a super fine structure with splitting width Δ. In order to investigate the effects of the splitting on the spontaneous emission spectrum in the PBG and free vacuum reservoirs, we adopt the first model as shown in Fig.1(a). We plot the spontaneous emission spectrum as a function of detuning δ_k in the three cases as shown in Fig.2. From Figs.2(b) and 2(c), we see that the spontaneous emission peaks

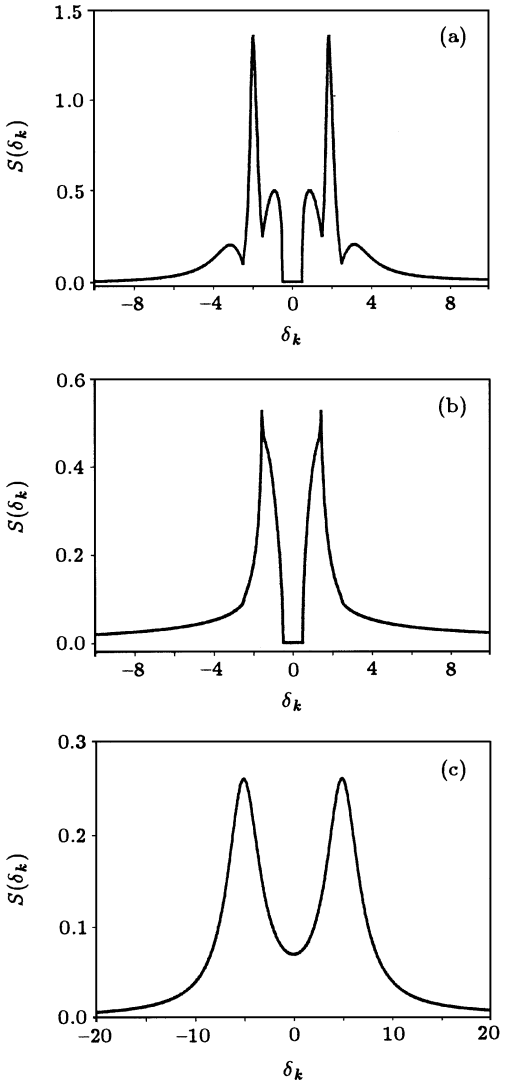


Fig.2. The spontaneous emission spectrum $S(\delta_k)$ (in arbitrary units) as a function of detuning δ_k in the case of Fig.1 (a). (a) For double-band isotropic PBG reservoir, β_{21}=1.0, Δ=2.0. (b) For double-band anisotropic PBG reservoir, α_{21}^2=1.0, Δ=2.0. (c) For free vacuum reservoir, γ_{21}=1.0, Δ=10.0. The other parameters used are A_{20}=1.0, $\delta_{c2c1}=1.0$, $\delta_{2c1}=0.5$. All parameters from Figs.2–5 are in units of β_{20}, α_{20}^2 and γ_{20} for isotropic PBG modes, anisotropic PBG modes and free vacuum modes, respectively.

correspond to the resonant transitions from the upper level to the lower two levels. This is expected and understandable for the splitting changes the resonant positions of the atomic transitions in both cases of the anisotropic PBG and free vacuum reservoirs. However, for the case of isotropic PBG reservoir (Fig.2(a)), the effect of the splitting width Δ on the spontaneous emission spectrum is quite different. It is seen that additional and unexpected peaks appear besides the peaks corresponding to the resonant transitions from the upper level to the lower levels. In order to investigate this new feature in the isotropic PBG reservoir, we plot the spontaneous emission spectra for different splitting widths Δ as shown in Fig.3, for different widths of forbidden gaps as shown in Fig.4 and different detuning of the upper level from the lower edge of the forbidden gap as shown in Fig.5. From Fig 2(a) and Figs.3–5, it is seen that the detuning for these additional peaks covers two ranges: from $\Delta - \frac{1}{2}\delta_{c2c1}$ to $\Delta + \frac{1}{2}\delta_{c2c1}$ and from $-\Delta - \frac{1}{2}\delta_{c2c1}$ to $-\Delta + \frac{1}{2}\delta_{c2c1}$, and is unconcerned with other parameters. The origin for this feature can be traced back to Eqs.(16), (17), (19), and (22). From these equations, the forms of Laplace transform of the delayed Green function involved in the spontaneous emission spectrum include the following items:

$$\left(\frac{\mathrm{i}}{\sqrt{\delta_k + \frac{1}{2}(\delta_{c2c1} - \Delta)}} + \frac{1.0}{\sqrt{\delta_k - \frac{1}{2}(\delta_{c2c1} + \Delta)}} \right)$$

and

$$\left(\frac{\mathrm{i}}{\sqrt{\delta_k - \frac{1}{2}(\delta_{c2c1} - \Delta)}} + \frac{1.0}{\sqrt{\delta_k + \frac{1}{2}(\delta_{c2c1} + \Delta)}} \right).$$

The above items show clearly that the splitting of the atomic ground state induces additional singularities of Laplace transform of the delayed Green function for isotropic PBG modes. These additional singularities occur at $\Delta - \frac{1}{2}\delta_{c2c1}$, $\Delta + \frac{1}{2}\delta_{c2c1}$, $-\Delta - \frac{1}{2}\delta_{c2c1}$ and $-\Delta + \frac{1}{2}\delta_{c2c1}$. It shows conclusively that the peaks resulting from the splitting of the atomic ground state stem from the contribution of the splitting to the Laplace transform of the delayed Green function of the isotropic PBG modes.

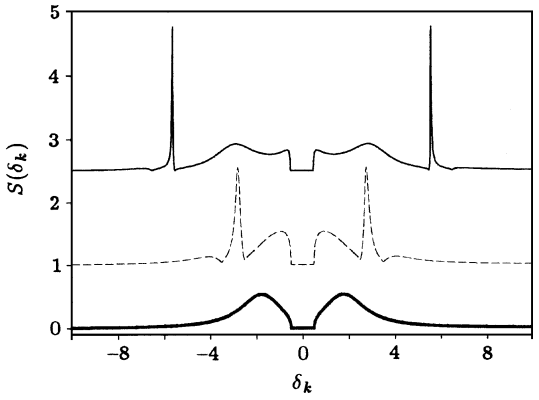


Fig.3. The spontaneous emission spectrum $S(\delta_k)$ (in arbitrary units) as a function of detuning δ_k for different splitting widths of the ground state levels in the case of double-band isotropic PBG reservoir. A_{20}=1.0, β_{21}=1.0, $\delta_{c2c1} = 1.0$, $\delta_{2c1} = 0.5$, and Δ=0.0, 3.0, 6.0 corresponding to thick solid line, short dashed line and thin solid line, respectively.

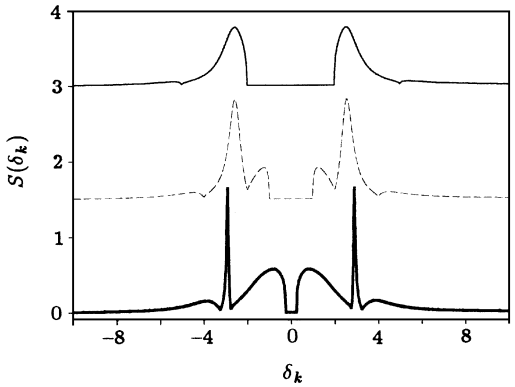


Fig.4. The spontaneous emission spectrum $S(\delta_k)$ (in arbitrary units) as a function of detuning δ_k for the different forbidden gap widths in the case of the isotropic PBG reservoir. A_{20}=1.0, Δ=3.0, δ_{c2c1}=0.5, 2.0, 4.0 correspond to thick solid line, short dashed line and thin solid line, respectively, and $\delta_{2c1} = \frac{1}{2}\delta_{c2c1}$.

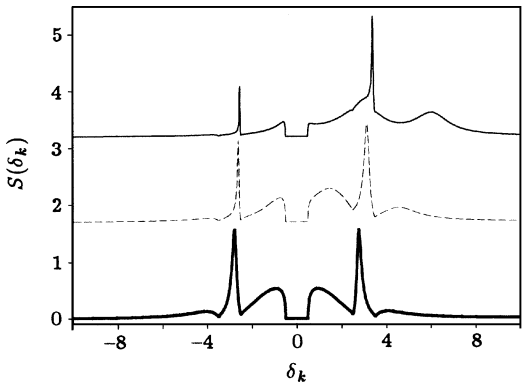


Fig.5. The spontaneous emission spectrum $S(\delta_k)$ (in arbitrary units) as a function of detuning δ_k for different detuning of the upper level $|2\rangle$ from the lower edge of the forbidden gap in the case of the isotropic PBG reservoir. A_{20}=1.0, Δ=3.0, $\delta_{c2c1} = 1.0$, δ_{2c1}=0.5, 2.0, 4.0 correspond to thick solid line, short dashed line and thin solid line, respectively.

3.2. Quantum interference in spontaneous emission spectrum

In the first model, quantum interferences cannot be considered because there is only one upper level. In order to compare with the spontaneous emission and investigate quantum interferences, we adopt the second model as shown in Fig.1(b). We study first the case where an atom is equally and synchronously pumped to the upper levels, employing symmetric

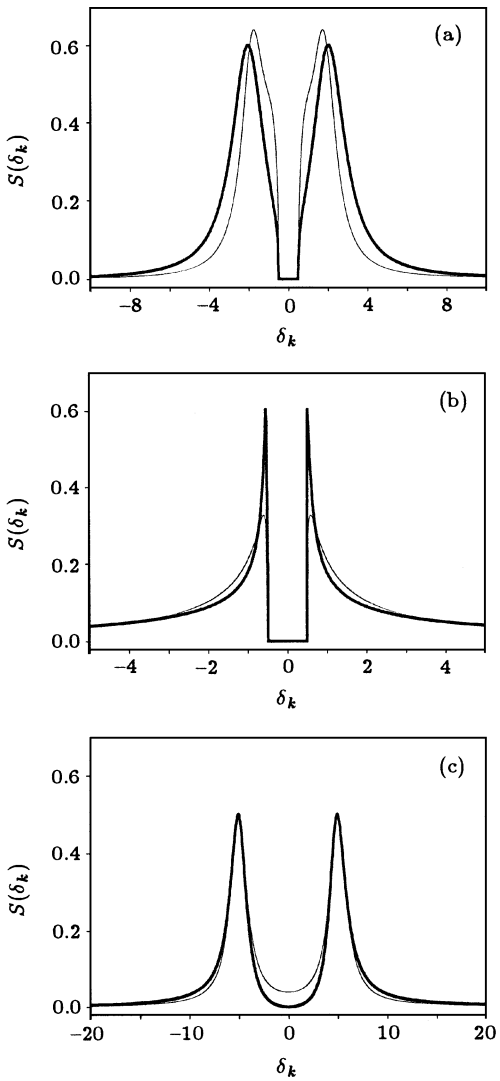


Fig.6. The spontaneous emission spectrum $S(\delta_k)$ (in arbitrary units) as a function of detuning δ_k. (a) Double-band isotropic PBG reservoir and $\beta_{20} = 1.0$, (b) double-band anisotropic PBG reservoir and $\alpha_{20}^2 = 1.0$, (c) free vacuum reservoir and $\omega_{32} = 10.0, \gamma_{20} = 1.0$. The other parameters used are A_{20}=0.5, A_{30}=0.5, $\delta_{c2c1} = 1.0$, $\delta_{30c2} = 0.5$, $\delta_{20c1} = -0.5$ and $\eta_{32} = 0$ (for thin solid lines), $\eta_{32} = 1.0$ (for thick solid lines). All parameters from Figs.6 and 7 are in units of β_{30}, α_{30}^2 and γ_{30} for isotropic PBG modes, anisotropic PBG modes and free vacuum modes, respectively, except that η_{32} is dimensionless.

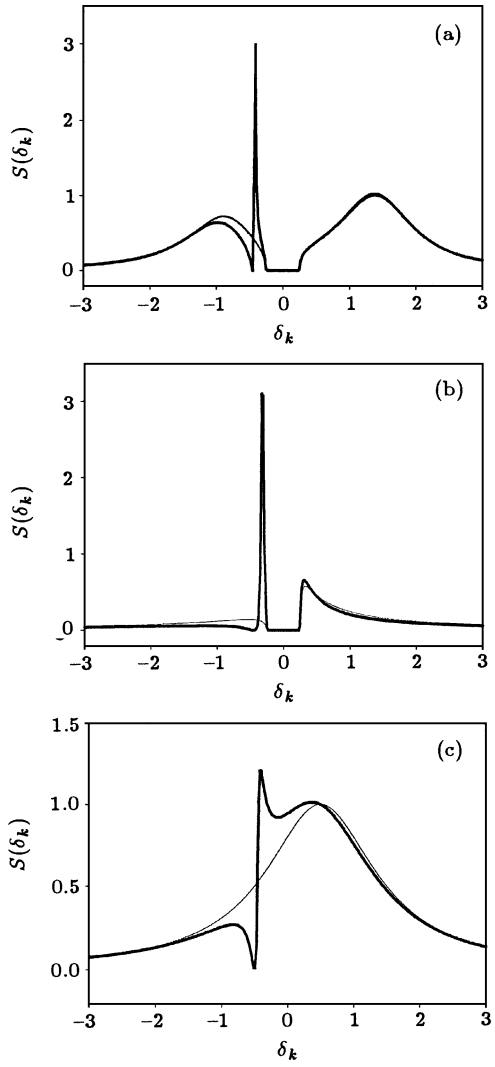


Fig.7. The spontaneous emission spectrum $S(\delta_k)$ (in arbitrary units) as a function of detuning δ_k. (a) Double-band isotropic PBG reservoir and $\beta_{20} = 0.1$, (b) double-band anisotropic PBG reservoir and $\alpha_{20}^2 = 0.1$, (c) free vacuum reservoir and $\omega_{32} = 1.0$, $\gamma_{20} = 0.1$. The other parameters used are A_{20}=0.0, A_{30}=1.0, $\delta_{c2c1} = 0.5$, $\delta_{30c2} = 0.2$, $\delta_{20c1} = -0.2$, $\eta_{32} = 0$ (for thin solid lines), $\eta_{32} = 1.0$ (for thick solid lines).

values of parameters for the two transitions. In Figs.6(a), 6(b) and 6(c), the spontaneous emission spectra are shown for the cases of isotropic PBG reservoir, anisotropic PBG reservoir, and free-space vacuum reservoir, respectively. It is seen that the quantum interferences have weaker effects on the spontaneous emission spectrum in these cases. If an atom is assumed to be initially pumped to level $|3\rangle$ with asymmetric parameters for the two atomic transitions, the ensuing emissions are seen to present a different picture with prominent features as shown in Fig.7. The quantum interferences induce a narrow spectral line, positioning near the transition frequency from

the empty upper level $|2\rangle$ to lower level $|0\rangle$. The origin for this new narrow spectral line has been analysed in detail in our previous paper.[47] It is that the quantum interferences induce a population transfer from level $|3\rangle$ to empty level $|2\rangle$ while the emission interferences of population from upper levels to the lower level are destructive. Hence, the narrow spectral lines are seen to arise from a population transfer under destructive emission interferences.

4. Conclusion

The two more realistic models have been adopted in this paper. The models assume three-level atomic transitions interacting with the same reservoir which are in turn the isotropic PBG modes, the anisotropic PBG modes and the free vacuum modes. The results of spontaneous emission in the two models are compared. The effects of the splitting of atomic ground state levels and the quantum interferences on spontaneous emission spectra have been discussed in the two model systems. In the case of isotropic PBG modes, the splitting of the atomic ground state induces new emission spectral lines because of its contribution to Laplace transform of the delayed Green function. The quantum interferences can induce a transfer of population between the two upper levels, resulting in additional emission spectral lines under destructive emission interferences.

References

[1] Zhou P and Swain S 1997 *Phys. Rev. Lett.* **78** 832
[2] Zhou P and Swain S 1997 *Phys. Rev.* A **56** 3011
[3] Zhu S Y 1995 *Phys. Rev.* A **52** 710
[4] Keitel C H 1999 *Phys. Rev. Lett.* **83** 1307
[5] Zhu S Y and Scully M O 1996 *Phys. Rev. Lett.* **76** 388
[6] Zhou P and Swain S 1996 *Phys. Rev. Lett.* **77** 3995
[7] Radmore P M and Knight P L 1982 *J. Phys.* B **15** 561
[8] Agarwal G S 1974 *Quantum Optics* (Berlin: Springer)
[9] Berman P R 1998 *Phys. Rev.* A **58** 4886
[10] Lee H, Polynkin P, Scully M O and Zhu S Y 1997 *Phys. Rev.* A **55** 4454
[11] Paspalakis E, Kylstra N J and Knight P L 1999 *Phys. Rev. Lett.* **82** 2079
[12] Paspalakis E and Knight P L 1998 *Phys. Rev. Lett.* **81** 293
[13] Scully M O, Zhu S Y and Gavrielides A 1989 *Phys. Rev. Lett.* **62** 2813
[14] Agarwal G S and Menon S 2001 *Phys. Rev.* A **63** 023818
[15] Agarwal G S and Patnaik A K 2001 *Phys. Rev.* A **63** 043805
[16] Mavroyannis C 2001 *J. Opt.* B: *Quantum Semiclass. Opt.* **2** 735
[17] Li G X, Li F L and Zhu S Y 2001 *Phys. Rev.* A **64** 013819
[18] Li G, Wu S and Zhou P 2001 *Eur. Phys. J.* D **15** 267
[19] Gao S Y, Li F L and Zhu S Y 2002 *Phys. Rev.* A **66** 043806
[20] Ficek Z and Swain S 2002 *J. Mod. Opt.* **49** 3
[21] Paspalakis E and Knight P L 2002 *Phys. Rev.* A **66** 015802
[22] Paspalakis E and Knight P L 2002 *J. Opt.* B: *Quantum Semiclass. Opt.* **4** s392
[23] Paspalakis E and Knight P L 2002 *J. Mod. Opt.* **49** 87
[24] Woldeyohannes M and John S 1999 *Phys. Rev.* A **60** 5046
[25] Lambropoulos P, Nikolopoulos G M, Nielsen T R and Bat S 2000 *Rep. Prog. Phys.* **63** 455
[26] Yablonovitch E 1987 *Phys. Rev. Lett.* **58** 2059
[27] John S 1987 *Phys. Rev. Lett.* **58** 2486
[28] John S and Quang T 1995 *Phys. Rev.* A **50** 1764
[29] John S and Wang J 1991 *Phys. Rev.* B **43** 12772
[30] Nikolopoulos G M and Lambropoulos P 2000 *Phys. Rev.* A **61** 053812
[31] Kofman A G, Kurizki G and Sherman B 1994 *J. Mod. Opt.* **41** 353
[32] Bay S, Lambropoulos P and Molmer K 1997 *Phys. Rev.* A **55** 1485
[33] Zhu S Y, Chen H and Huang H 1997 *Phys. Rev. Lett.* **79** 205
[34] Yang Y P and Zhu S Y 2000 *Phys. Rev.* A **61** 043809
[35] Yang Y P and Zhu S Y 2000 *J. Mod. Opt.* **47** 1513
[36] Zhu S Y, Yang Y P, Chen H, Zheng H and Zubairy M S 2000 *Phys. Rev. Lett.* **84** 2136
[37] Yang Y P, Lin Z X, Zhu S Y, Chen H and Feng W 2000 *Phys. Lett.* A **270** 41
[38] Paspalakis E, Kylstra N J and Knight P L 1999 *Phys. Rev.* A **60** R33
[39] Angelakis D G, Paspalakis E and Knight P L 2001 *Phys. Rev.* A **64** 013801
[40] Konopka M 1999 *Phys. Rev.* A **60** 4183
[41] Lewenstein M and Rzazewski K 2000 *Phys. Rev.* A **61** 022105
[42] Vats N and John S 1998 *Phys. Rev.* A **58** 4168
[43] Yang Y P, Lin Z X, Zhu S Y, Chen H and Feng W G 2000 *Phys. Lett.* A **41** 270
[44] Petrosyan D and Kurizki G 2001 *Phys. Rev.* A **64** 023810
[45] Jack M W and Hope J J 2001 *Phys. Rev.* A **63** 043803
[46] Xic S Y, Yang Y P and Wu X 2001 *Eur. Phys. J.* D **13** 129
[47] Zhang H Z, Tang S H, Dong P and He J 2002 *Phys. Rev.* A **65** 063802
[48] Zhang H Z, Tang S H, Dong P and He J 2002 *J. Opt.* B: *Quantum Semiclass. Opt.* **4** 300
[49] Zhang H Z, Yang J B and Tang S H 2003 *J. Mod. Opt.* **50** 1649